DEUTSCHES ELEKTRONEN – SYNCHROTRON DESY

DESY 89-120
September 1989

Energy-Level Statistics of the Hadamard-Gutzwiller Ensemble

R. Aurich, F. Steiner
II. Institut für Theoretische Physik, Universität Hamburg

ISSN 0418-9833

NOTKESTRASSE 85 · 2 HAMBURG 52

To be sure that your preprints are promptly included in the
HIGH ENERGY PHYSICS INDEX,
send them to the following address (if possible by air mail):

DESY
Bibliothek
Notkestrasse 85
2 Hamburg 52
Germany

DESY 89–120
September 1989

ISSN 0418 – 9833

Energy–Level Statistics of the Hadamard–Gutzwiller Ensemble [1]

by

R.Aurich and F.Steiner

II.Institut für Theoretische Physik , Universität Hamburg
Luruper Chaussee 149 , 2000 Hamburg 50
Federal Republic of Germany

Abstract

The statistical properties of the quantal energy levels of the *Hadamard–Gutzwiller ensemble* – whose classical members belong to the class of systems with *hard chaos* – are investigated. Based on a sample of 4500 energy levels, it is shown that the short–range statistics as nearest–neighbour spacing distributions are governed by the GOE predictions of random–matrix theory, which was first surmised by Wigner and by Landau and Smorodinsky for nuclear level statistics. This result strengthens the hypothesis, that quantum systems with chaotic classical counterpart display level repulsion as predicted by random–matrix theory. However, the level statistics describing correlations over greater level distances deviate from the GOE predictions, which is explained as a simple consequence of the fact that the spectral rigidity $\Delta_3(L)$ introduced by Dyson and Mehta saturates non–universally at a finite value Δ_∞ for $L \to \infty$ in complete agreement with the semiclassical theory developed by Berry.

Submitted to Physica D

[1] Supported by Deutsche Forschungsgemeinschaft under Contract No. DFG–Ste 241/4–2

I Introduction

It is now commonly believed that the generic systems in classical physics are not the standard "text-book systems", which are completely integrable, but the non-integrable or so-called *chaotic* systems. The latter display a very strong dependence on the initial conditions, i. e. even extremely small perturbations have exponentially growing effects on the time-evolution of the systems. The chaotic behaviour of such systems arises from the non-linearity of the differential equations describing them. But this non-linearity is missing in quantum mechanics, because the corresponding differential equation is the Schrödinger equation, which is linear and seems to smooth out the chaos observed in the classical realm. Nevertheless, there is the hope that the *statistical properties* of the quantal energy spectra show a clear sign of chaos. It has been conjectured [1,2,3] that the statistical properties can be described by random-matrix theory, originally proposed by Wigner and by Landau and Smorodinsky for a better understanding of the energy levels of complex nuclei (for a collection of the original papers, see [4]). The random-matrix theory [5] asserts that the statistical properties of the nuclear levels are the same as for the eigenvalues of random matrices of the Gaussian orthogonal ensemble (GOE), which should be applied for systems with time-reversal symmetry. The GOE, which is invariant under orthogonal transformations, consists of real symmetric matrices, whose matrix elements are zero-centered Gaussian distributed. For systems without time-reversal symmetry, one expects statistical properties according to the Gaussian unitary ensemble (GUE), which is invariant under unitary transformations.

The nuclear level statistics are in good agreement with the GOE predictions [4,6,7,8,9], and it is conjectured [1,2,3] that these properties are common to the much wider class of chaotic systems in general, whereas a Poisson distributed spectrum is expected for integrable systems. (For recent reviews, see e. g. refs. [10,11,12,13].) To check this assumption one needs a large number of eigenvalues for a given system, whose chaotic nature can be proved rigorously. Problems arise from the numerical point of view, because it is notoriously difficult to compute enough eigenvalues for chaotic systems with the accuracy required to get significant statistics.

Following the spirit of random-matrix theory, it is natural to improve the situation by considering not just a *single* chaotic system, but rather an *ensemble* of chaotic systems belonging to a certain family of systems sharing common properties. (For a similar approach see [27] for complex atomic spectra and [7] for the "nuclear data ensemble".) By computing the lower part of the quantal energy spectrum for as many members of the ensemble as needed for statistical significance, one avoids the serious problem of calculating very high energy levels. Since it is known that the properties of nuclear level statistics are approximately independent of the energy range, i. e. the ground state domain shows the same behaviour as very high energy ranges [6], one can suppose, that the results obtained for the low energy spectra of the ensemble are valid in a much wider energy range, perhaps even in the semiclassical region.

Adopting this strategy, we study in this paper the energy-level statistics of the *Hadamard-Gutzwiller ensemble.* The Hadamard-Gutzwiller *model* [14,15] has been the subject of our earlier detailed investigations [16,17,18], where the emphasis has been on the Selberg trace formula, which for this model is identical to Gutzwiller's periodic-orbit theory [19,20]. In ref.[18] we studied a very special version of this model, called the *symmetrical* Hadamard-Gutzwiller model, which is defined by choosing the most symmetrical fundamental region in the Poincaré disc (i. e. a regular octagon) for the Riemann surface of genus two, on which the particle motion takes place. For this model the level statistics did not show the expected GOE behaviour even after desymmetrization [18]. However, there is an infinite number of inequivalent compact Riemann surfaces of genus two, i. e. there exists an infinite family of Hadamard-Gutzwiller models, which we call the Hadamard-Gutzwiller *ensemble.* We suspected that the symmetrical Hadamard-Gutzwiller model, studied in [18], is a very special member of the Hadamard-Gutzwiller ensemble, insofar as it possesses a very high symmetry leading to non-generic level statistics even after desymmetrization. On the other hand, it could be hoped that a generic member of the Hadamard-Gutzwiller ensemble, which is represented by an *asymmetrical*

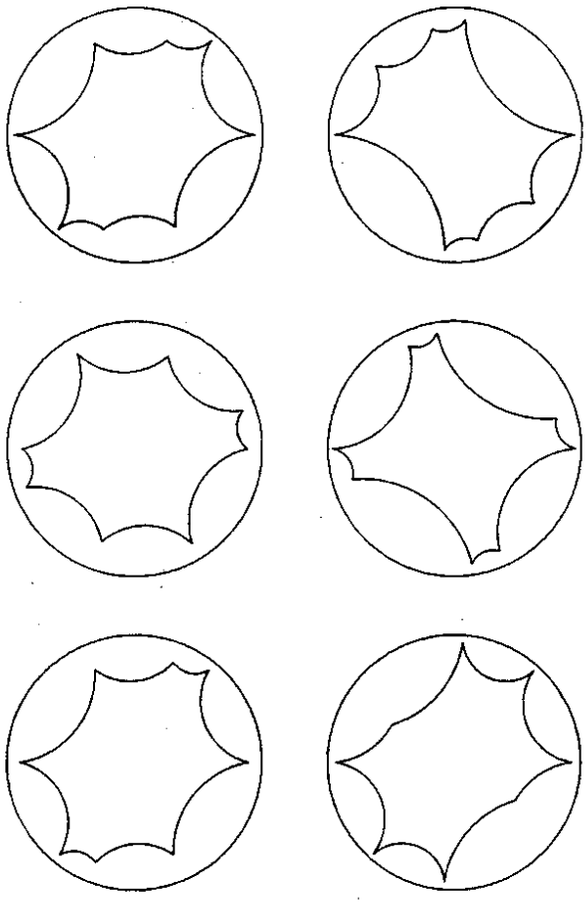

Figure 1: The fundamental regions of six members of the Hadamard–Gutzwiller ensemble are shown in the Poincaré disc.

octagon, would reveal the expected level statistics. This is indeed the case for the short–range correlations as will be shown in this paper. Working with a large ensemble (we use 30 different Riemann surfaces of genus two) we can base our statistical study on 4500 eigenvalues which is a reasonably large number, and allows us to make a detailed analysis of various statistical measures. Whereas the short–range statistics turn out to be in nice agreement with the GOE predictions, the long–range correlations show a different behaviour. This long–range behaviour can be completely understood in terms of a single parameter Δ_∞, which measures the asymptotic value of the Δ_3–statistics of Dyson and Mehta [21]. We thus obtain a coherent picture of the energy–level statistics of the Hadamard–Gutzwiller ensemble.

Our paper is organized as follows. After describing the Hadamard–Gutzwiller ensemble and the construction of its members in sect.II and III, respectively, we turn in sect.IV to the energy–level statistics. In contrast to the usual approach we begin with the functions $E(k, L)$ introduced by Mehta and Cloizeaux [22], describing the probability that a randomly chosen energy interval of length L contains k levels, which are more fundamental than the following statistics, because the latter can be derived from the former. Then we discuss the higher moments of the number statistics $\Sigma^2(L), \gamma_1(L), \gamma_2(L)$, the level spacings $P(k, s)$ and finally the spectral rigidity $\Delta_3(L)$. We close with an explanation of our findings in terms of the saturation value Δ_∞ of the spectral rigidity $\Delta_3(L)$.

II The Chaotic Hadamard–Gutzwiller Ensemble

The Hadamard–Gutzwiller *model* [14,15] is a conservative Hamiltonian system with two degrees of freedom, which is strongly chaotic. It is defined on a compact Riemann surface with constant negative curvature with genus $g = 2$, on which the free motion of a point particle is considered. Genus $g = 2$ means that this surface is topologically a sphere with two handles, i. e. it looks like a double doughnut. For an excellent review see ref.[23].

Riemann surfaces of genus $g \geq 2$ can be parametrized by a $6g-6$ dimensional moduli space. In this way we get for $g = 2$ an *ensemble of purely chaotic systems*, whose members can be described as points in a 6 dimensional moduli space. However, in contrast to genus $g = 1$, where the moduli space is explicitly known (the $SL(2,\mathbf{Z})$ fundamental domain in the complex upper half plane), for our ensemble of genus $g = 2$ it is not the case. Therefore, we proceed in the following way. The double doughnut can be cut so that one obtains an octagon with geodesic edges, where opposite sides must be identified, which leads to periodic boundary conditions. The octagon is mapped into the Poincaré disc, which consists of the interior of the unit circle in the complex z–plane ($z = x_1 + ix_2$) endowed with the hyperbolic metric

$$g_{ij} = \frac{4}{(1-x_1^2-x_2^2)^2}\delta_{ij} \ , \ i,j = 1,2 \tag{1}$$

corresponding to constant negative Gaussian curvature $K = -1$. In the Poincaré disc, geodesics are circles intersecting the boundary of the disc perpendicularly. The classical motion is determined by the Hamiltonian $H = \frac{1}{2m}p_i g^{ij} p_j$, $p_i = m\, g_{ij}\, dx^j/dt$, while the quantum mechanical system is governed by the *Schrödinger equation*

$$-\Delta\Psi_n(z) = E_n\Psi_n(z) \quad , \quad \text{with} \quad \Delta = \frac{1}{4}(1-x_1^2-x_2^2)^2\left(\frac{\partial^2}{\partial x_1^2}+\frac{\partial^2}{\partial x_2^2}\right) \quad , \tag{2}$$

where we used $\hbar = 2m = 1$.

The periodic boundary conditions are realized by identifying the points z and $b(z)$,

$$z' = b(z) := \frac{\alpha z+\beta}{\beta^* z+\alpha^*} \quad , \quad |\alpha|^2-|\beta|^2 = 1 \quad , \tag{3}$$

where the "boosts"

$$b = \begin{pmatrix} \alpha & \beta \\ \beta^* & \alpha^* \end{pmatrix} \in \mathrm{SU(1,1)}/\{\pm 1\}$$

are chosen such that they map a given edge onto the opposite edge. One needs 4 boosts for each octagon, and each octagon of the ensemble has different boosts because of their different shapes.

As an example, we present in fig.1 the fundamental regions of 6 members of the Hadamard–Gutzwiller ensemble. Notice that all octagons have the same (non–euclidean) area $A = 4\pi$ as follows from the Gauß–Bonnet theorem $A = 4\pi(g-1)$ for $g = 2$.

Let us consider an arbitrary member of the Hadamard–Gutzwiller ensemble (HGE), which is uniquely defined by its fundamental region (octagon) F and the associated 4 boosts as described above. Denote by Δ_F the Laplace–Beltrami operator defined in eq.(2), where the index F indicates that Δ_F is defined by acting on wavefunctions $\Psi_n(z), z \in F$, satisfying periodic boundary conditions on ∂F. The HGE is then defined by the set $\{\widehat{H}_F\}$ of all Hamiltonians $\widehat{H}_F = -\Delta_F$, where F runs through all fundamental regions corresponding to the 6–dimensional moduli space. Each member $\widehat{H}_F$ has a different (discrete) energy spectrum $0 = E_0^F < E_1^F \leq E_2^F \leq \ldots$ due to the different shapes of the octagons F. However, Weyl's law $E_n^F \sim \frac{4\pi}{A}n$, $n \to \infty$, is the same for all of them, since it is only determined by their area $A = 4\pi$, i.e. the n–th quantal energy is approximately $E_n^F \sim n$. The statistical analysis carried out in sect.IV is concerned with the *fluctuations* of the energies $\{E_n^F\}$ around this mean.

III Construction of the Octagons

It is always possible to map the octagons into the Poincaré disc in such a way , that their boundaries are invariant under the reflection $z \to -z$. Fixing three adjacent corners at z_1, z_2 and z_3 defines an octagon, see fig.2. The six degrees of freedom in choosing the three complex numbers z_1, z_2 and z_3 correspond to the 6 dimensions of the moduli space. Reflection at the origin yields immediately the

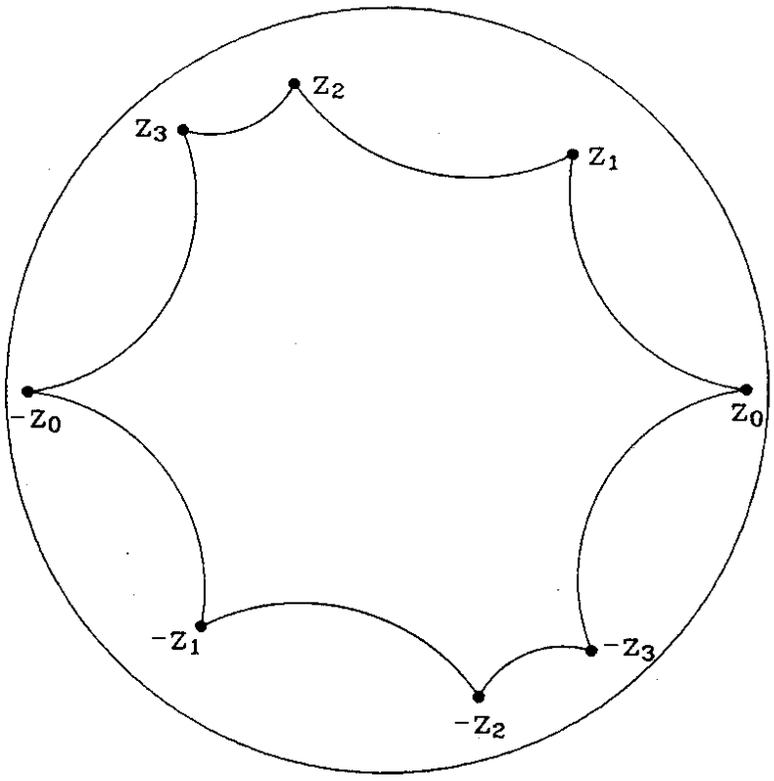

Figure 2: Example of an asymmetric octagon in the Poincaré disc with the defining points z_1, z_2 and z_3 as explained in the text.

three further corners at $-z_1, -z_2$ and $-z_3$. The missing two corners, z_0 and $-z_0$, say, are determined by the fact, that the area of the octagon must be $A = 4\pi$.

The last task is to determine the 4 boosts needed for implementing the periodic boundary conditions. Consider for example the boost b, which maps the edge between $-z_1$ and $-z_2$ onto that between z_1 and z_2. The two conditions $b(-z_2) = z_1$ and $b(-z_1) = z_2$ give

$$\begin{aligned} \alpha^* z_1 + \alpha z_2 - \beta^* z_1 z_2 - \beta &= 0 \\ \alpha^* z_2 + \alpha z_1 - \beta^* z_1 z_2 - \beta &= 0 \end{aligned}$$

which yield immediately Im $\alpha = 0$, and with the normalization $|\alpha|^2 - |\beta|^2 = 1$, $\alpha = \sqrt{1+|\beta|^2}$ and

$$\sqrt{1+|\beta|^2}(z_1 + z_2) - \beta^* z_1 z_2 - \beta = 0 \quad . \tag{4}$$

The last equation and analogous ones for the other edges determine the boosts.

IV The Statistical Properties of the Quantal Energies

The quantal energies for a given octagon are determined by the Schrödinger equation (2) with the periodic boundary conditions that points z, z' on opposite edges must be identified via $z' = b_i(z)$, where b_i maps the edge belonging to z onto that of z'. The problem is well defined, and we use the finite–element method for solving the Schrödinger equation as explained in our earlier paper [18]. The finite–element method is based on a variational principle and yields therefore upper bounds for the quantal energies. Using fourth–order polynomials as ansatz functions and a tessellation of the octagon in triangles leading to matrices of dimension roughly 1300, we get the first 75 quantal energy levels with the required accuracy. The calculation was done on the Cray Y-MP at the HLRZ in Jülich.

Because both the Schrödinger equation (2) and the boundaries are invariant under the reflection $z \to -z$, the quantal energies belong to the two parity classes "+" for $\Psi(z) = \Psi(-z)$ and "–" for $\Psi(z) = -\Psi(-z)$. A generic octagon has no further symmetries. In order to study the statistics of

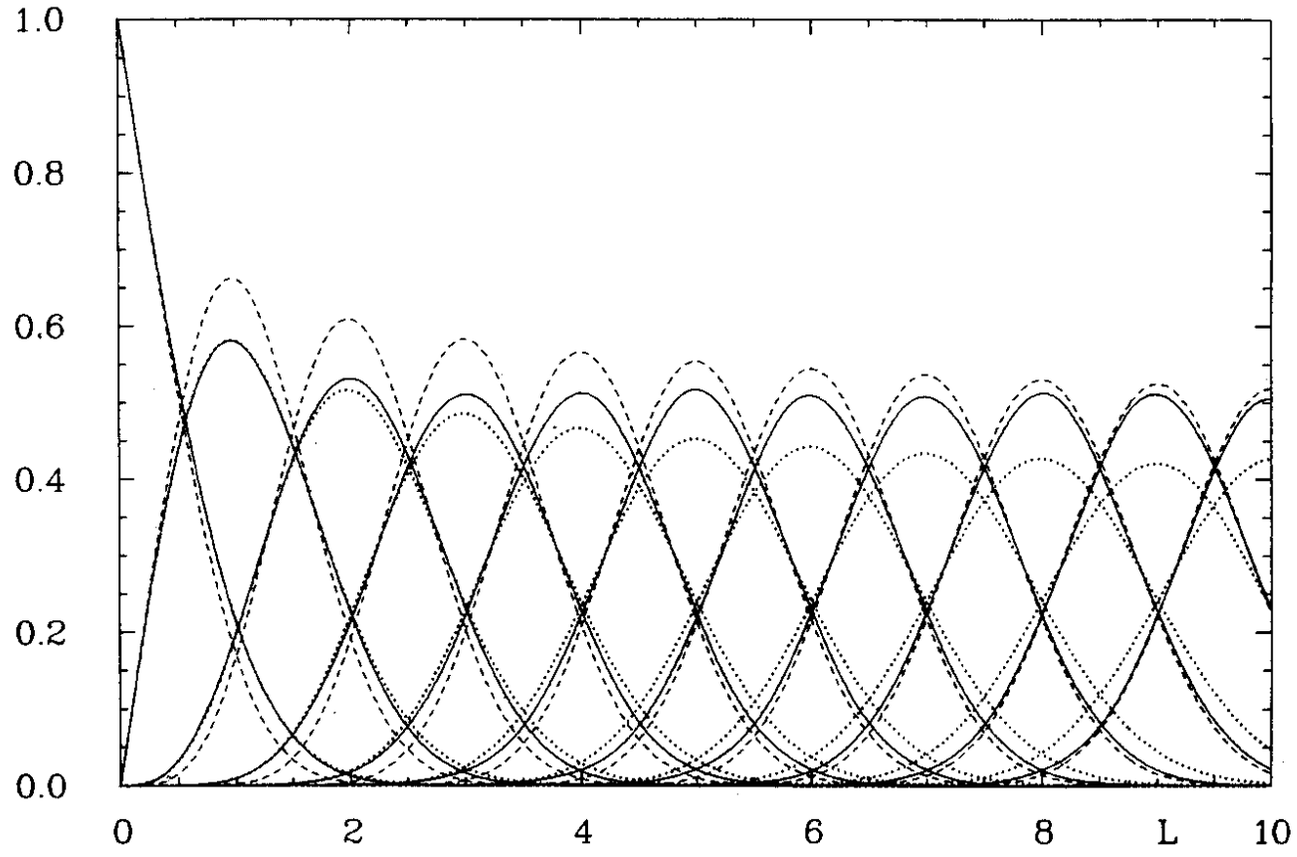

Figure 3: $E(k, L)$ for the Hadamard–Gutzwiller ensemble (full curve) for $k = 0$ to 10 in comparison with the GOE (dotted curve) and GUE (dashed curve) predictions. For a given value of k, $E(k, L)$ can be identified by its maximum approximately at $L = k$.

the energy spectra, one must consider the parity classes separately, because one is not interested in correlations due to this symmetry.

We constructed 30 asymmetric octagons, to be considered as random members of the Hadamard–Gutzwiller ensemble, and then calculated the first 75 quantal energies for each octagon and for each parity class. This yields 4500 energy levels, corresponding to 60 different spectra which are used in the following statistical studies of quantal energies, where one always performs averages over the ensemble. We assume that one has applied the process of unfolding to the individual quantal spectra, i. e. the mean spacing between two adjacent levels of a given sequence is normalized to unity.

IV.1 The Functions $E(k, L)$

Let us denote by $E(k, L)$, $k = 0, 1, 2, \ldots$ the probability [22], that a randomly chosen energy interval of length L contains exactly k levels. For a given value of k, the functions $E(k, L)$ have a maximum approximately at $L = k$, because of the normalization of the mean level spacing, and satisfy the normalization

$$\sum_{k=0}^{\infty} E(k, L) \;=\; 1 \quad . \tag{5}$$

Other statistics like $\Sigma^2, \gamma_1, \gamma_2, \Delta_3$ and level–spacing statistics can be calculated from the knowledge of $E(k, L)$, which are in this sense more fundamental. The random matrix theory makes well–defined predictions for $E(k, L)$ in the case of GOE and GUE [22], see fig.3. (Ref.[22] contains tables and figures for $E(k, L)$ for $k = 0$ to 7 and $0 \leq L \leq 5.093$. The curves shown in fig.3 are the results of our own calculations which extend to $k = 13$ and $0 \leq L \leq 13$ [24].)

The function $E(0, L)$, which is the probability for finding no level in an interval of length L, starts with 1 at $L = 0$ and decreases very fast with increasing L. For the Poisson case one gets

	GOE				Hadamard-Gutzwiller ensemble				GUE			
k	α	β	γ	δ	α	β	γ	δ	α	β	γ	δ
1	0.924	0.004	0.993	0.996	0.818	0.195	0.864	0.916	0.563	0.467	0.853	0.864
2	1.029	0.551	0.216	2.728	0.767	1.260	0.204	1.902	0.633	1.064	0.166	2.871
3	1.097	1.137	0.009	5.012	0.706	2.451	0.048	2.332	0.671	1.720	0.004	5.645

Table 1: The parameters α, β, γ and δ for the ansatz $E(k,L) = \gamma L^{\delta} \exp(-(L-\beta)^2/2\alpha)$ for the Hadamard–Gutzwiller ensemble in comparison with the GOE and GUE predictions.

k	GOE	Hadamard-Gutzwiller ensemble	GUE
4	0.726	0.606	0.493
5	0.772	0.604	0.516
6	0.809	0.616	0.535
7	0.841	0.616	0.550
8	0.868	0.614	0.564

Table 2: The parameter α for the ansatz $E(k,L) = (2\pi\alpha)^{-1/2} \exp(-(L-k)^2/2\alpha)$ for the Hadamard–Gutzwiller ensemble in comparison with the GOE and GUE predictions.

$E_{\mathrm{Poisson}}(0,L) = e^{-L}$, whereas we get for the Hadamard–Gutzwiller ensemble (HGE) an excellent fit with

$$E(0,L) = \mathrm{erfc}(aL) := \frac{2}{\sqrt{\pi}} \int_{aL}^{\infty} dx\, e^{-x^2} \tag{6}$$

with $a_{\mathrm{HGE}} = 0.880$. This agrees well with the GOE prediction $a_{\mathrm{GOE}} = \frac{\sqrt{\pi}}{2} \simeq 0.88622\ldots$, if one assumes the Wigner surmise to be correct. The GUE prediction matches not so well with $\mathrm{erfc}(aL)$ and does not agree with $E_{\mathrm{HGE}}(0,L)$.

In order to compare $E_{\mathrm{HGE}}(k,L)$ with $E_{\mathrm{GOE}}(k,L)$ and $E_{\mathrm{GUE}}(k,L)$, we use simple fit functions and compare the fit parameters. For $k = 1$ to 3 we use the ansatz

$$E(k,L) = \gamma\ L^{\delta}\ \exp(-(L-\beta)^2/2\alpha) \tag{7}$$

to describe our data and the GOE and GUE curves, whereas for higher k values we fix $\beta = k$, $\gamma = \frac{1}{\sqrt{2\pi\alpha}}$ and $\delta = 0$, because the functions $E(k,L)$ agree well with the Gaussian normal distribution

$$E(k,L) = \frac{1}{\sqrt{2\pi\alpha}} \exp(-(L-k)^2/2\alpha)\ \ ,\ \ k = 4,5,\ldots\ . \tag{8}$$

(A possible dependence of the fit parameters on k is not explicitly written out.) The fit functions have to obey eq.(5), at least approximately. The ansatz (8) can be improved by including a correction term proportional to a parameter κ

$$E(k,L) = \left\{ \frac{1}{\sqrt{\pi 2\alpha}} - \kappa\alpha + \kappa(L-k)^2 \right\} \exp(-(L-k)^2/2\alpha)\ \ , \tag{9}$$

where κ is chosen such that the ansatz (9) optimally obeys eq.(5). We have checked, that this ansatz obeys eq.(5) almost perfectly for $\alpha > 0.25$. The error is less than 10^{-3} and 10^{-5} for $\alpha = 0.3$ and

0.6, respectively. However, with increasing $\alpha > 0.5$ the correction can be neglected and, indeed, the quality of our fit is independent of the choice between eq.(8) and eq.(9). Therefore, we choose eq.(8) for simplicity. The parameters are listed in table 1 and 2. (Here and in the following, our numerical values are presented with 3 decimal places, where, however, the last figure may be uncertain.) The "width" α of the Gaussian normal distribution increases for the Hadamard–Gutzwiller model very slowly with k until for $k = 4$ to 8 it saturates at a mean value $\alpha_\infty = 0.615$. The saturation of α for $k \rightarrow \infty$, which occurs neither in the GOE nor in the GUE case, will find a nice explanation in sect.IV.5. The α–values for the Hadamard–Gutzwiller ensemble lie always between the GOE and GUE predictions. For smaller k's a closer match is obtained in comparison with GOE than with GUE, but this reverses for greater k's, which indicates that the spectrum of our system is more rigid over greater "k–distances" than the GOE spectrum.

The functions $E(k, L)$ for the Hadamard–Gutzwiller ensemble (full curve), GOE (dotted curve) and GUE (dashed curve) are shown in fig.3. For small k's, a much closer match of $E_{\mathrm{HGE}}(k, L)$ with the GOE prediction is obtained than with those of GUE. With increasing k values, $E_{\mathrm{HGE}}(k, L)$ seems to approach the $E_{\mathrm{GUE}}(k, L)$ functions until for $k = 9, 10$ the agreement is nearly perfect. This is an accident, however, because the functions $E_{\mathrm{HGE}}(k, L)$ have already a constant width, whereas the widths of the functions $E_{\mathrm{GUE}}(k, L)$ are still increasing, and thus for $k = 9$ and 10 the widths of both are comparable just by chance.

The last point can be put on a more quantitative basis by anticipating the following relation

$$\alpha(k) \simeq \Sigma^2(k) \ , \ k > 1 \ , \tag{10}$$

which connects the "width" $\alpha = \alpha(k)$ of the function $E(k, L)$ with the number variance $\Sigma^2(L)$, defined in eq.(17) below, which is a measure for the local two–point fluctuations. Eq.(10) will be derived later in sect.IV.5 for the HGE as well as for GOE and GUE. But let us check already now the prediction (10) for GOE and GUE, which is possible since the random–matrix theory makes exact predictions for $\Sigma^2(L)$ [21]

$$\mathrm{GOE}: \quad \Sigma^2(L) = \frac{2}{\pi^2}\left[\ln(2\pi L) + \gamma_E + 1 - \frac{\pi^2}{8}\right] + O\left(\frac{1}{\pi^4 L^2}\right) \tag{11}$$

$$\mathrm{GUE}: \quad \Sigma^2(L) = \frac{1}{\pi^2}\left[\ln(2\pi L) + \gamma_E + 1\right] + O\left(\frac{1}{\pi^4 L^2}\right) \tag{12}$$

($\gamma_E = 0.5772\ldots$ is Euler's constant). In order to test our ansatz (8) together with the prediction (10), we have made a fit to the exact GOE and GUE predictions for $E(k, L)$ using (8) with $\alpha = \alpha(k) = \Sigma^2(k) + \varepsilon(k)$, where $\Sigma^2(k)$ is approximated by (11,12). As is seen in table 3, the values obtained for the "discrepancy" $\varepsilon(k)$, which is the only free parameter in our fit, are very small ($< 10^{-2}$) over the whole interval from $k = 1$ to 9, which is a nice confirmation of our ansatz (8) and our prediction (10), which can be written explicitly in the form ($k > 1$)

$$\begin{aligned} \alpha_{\mathrm{GOE}}(k) &\simeq \frac{2}{\pi^2}\left[\ln(2\pi k) + \gamma_E + 1 - \frac{\pi^2}{8}\right] \\ \alpha_{\mathrm{GUE}}(k) &\simeq \frac{1}{2}\alpha_{\mathrm{GOE}}(k) + \frac{1}{8} \ . \end{aligned} \tag{13}$$

For $k = 5$ we obtain from eq.(13) $\alpha_{\mathrm{GUE}}(5) \simeq 0.51$ and $\alpha_{\mathrm{GOE}}(5) \simeq 0.77$, and thus $\alpha_{\mathrm{GUE}} < \alpha_{\mathrm{HGE}} < \alpha_{\mathrm{GOE}}$ at this k value. But since for $k \rightarrow \infty$ $\alpha(k)$ saturates at a constant value α_∞ for the Hadamard–Gutzwiller ensemble, whereas it increases logarithmically for GOE and GUE, the difference in the level statistics between GOE and HGE is getting larger, while there must be a "crossover region" where the level statistics of the HGE approaches the GUE predictions. To determine the k value at which this crossover occurs, we demand $\alpha_{\mathrm{GUE}} = \alpha_\infty \simeq 0.6$. For $k = 9, 10, 11$ and 12 we obtain the values 0.57,0.58,0.59 and 0.60 for $\alpha_{\mathrm{GUE}}(k)$, which nicely confirms the results of fig.3 where one

observes good agreement between $E_{\mathrm{HGE}}(k,L)$ and $E_{\mathrm{GUE}}(k,L)$ for $k = 9$ and 10. But it is now obvious that this agreement is accidental, being simply caused by a crossover of the α_{GUE} and the α_{HGE} curves near $k = 12$.

k	GOE	GUE
1	0.039	0.012
2	-0.004	0.003
3	0.000	0.006
4	0.002	0.007
5	0.003	0.007
6	0.004	0.007
7	0.005	0.007
8	0.004	0.007

Table 3: The discrepancy $\varepsilon(k) := \alpha(k) - \Sigma^2(k)$ for the GOE and GUE predictions as explained in the text.

In sect.IV.5 we will need the integral $I(k)$ over the $E(k,L)$ functions, which has been introduced in [25]

$$I(k) \;=\; \int_0^\infty dL\; E(k,L) \quad . \tag{14}$$

Assuming the Gaussian behaviour (8), we obtain

$$I(k) \;=\; 1 \quad \text{for} \quad k \;=\; 4,5,\ldots \tag{15}$$

In table 4 we give the values for $I(k)$ obtained from the exact GOE and GUE predictions in comparison with the results for the HGE. It is seen that $I(k)$ saturates, indeed, in all three cases at the value 1 for $k \geq 4$.

k	GOE	HGE	GUE
0	0.643	0.641	0.590
1	0.923	0.909	0.944
2	0.975	0.975	0.986
3	0.989	0.983	0.994
4	0.994	0.996	0.997
5	0.996	1.000	0.998
6	0.997	1.000	0.999

Table 4: $I(k)$ for the Hadamard–Gutzwiller ensemble in comparison with the GOE and GUE predictions.

In summary, we observe, that for the Hadamard–Gutzwiller ensemble the $E(k,L)$ statistics for small k, testing the low–range statistics, agrees well with the GOE predictions, whereas statistics measuring properties over greater level distances show a more rigid spectrum. This property will also appear in the other statistics, measuring a wide enough level range, as $\Sigma^2(L)$, the level spacings $P(k,s)$ and the spectral rigidity $\Delta_3(L)$.

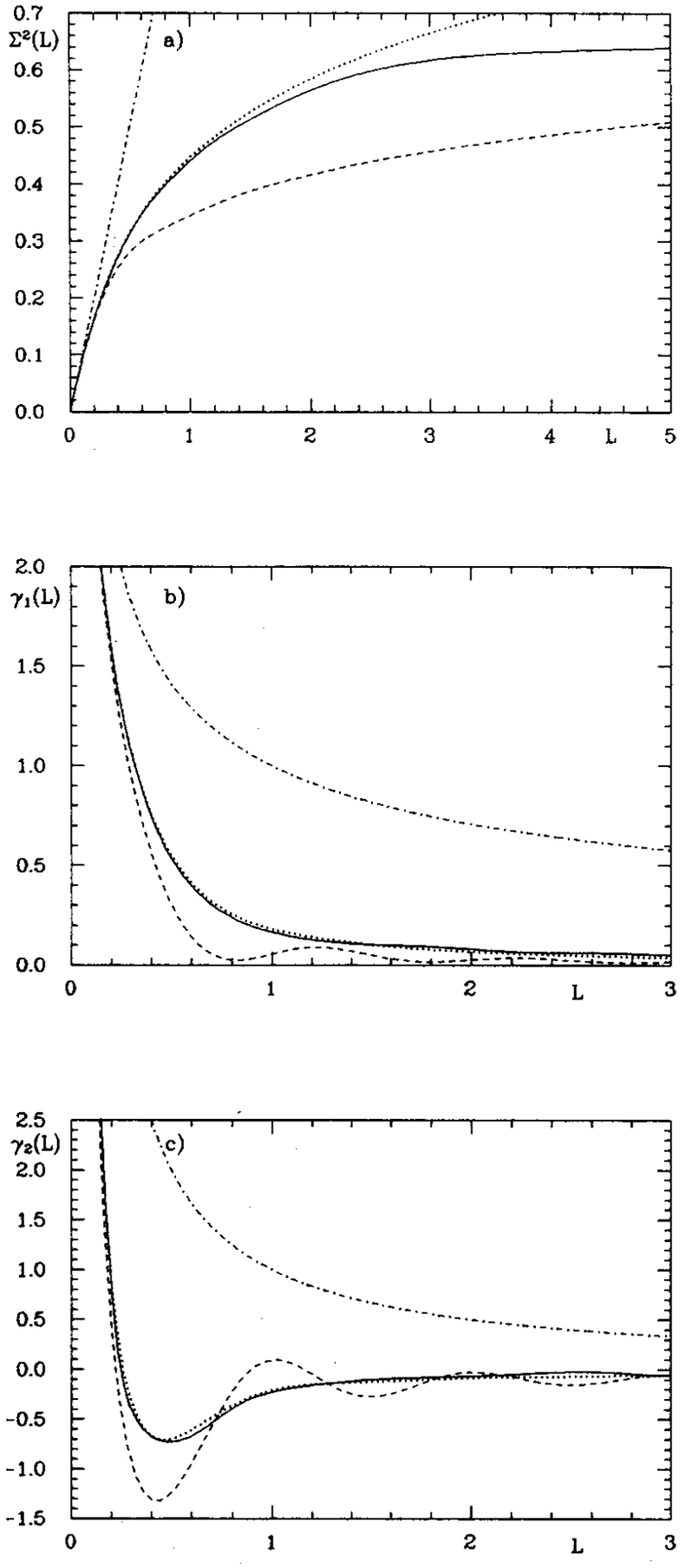

Figure 4: The higher moments $\Sigma^2(L)$ (a) , $\gamma_1(L)$ (b) and $\gamma_2(L)$ (c) of the number statistics $n(L)$ are presented. The full curves are obtained for the Hadamard–Gutzwiller ensemble, whereas the dotted curves belong to GOE, dashed curves to GUE and chain curves to Poisson spectra.

IV.2 Higher Moments of the Number Statistics $n(L)$

Let us denote by $n(L)$ the number of levels in an interval of length L. Its expectation value is

$$< n(L) > \; = \; \sum_{k=1}^{\infty} k\, E(k,L) \; = \; L \quad . \tag{16}$$

The interesting measures are the higher moments of $n(L)$, i. e. the number variance $\Sigma^2(L)$, the skewness γ_1 and the excess γ_2 which are connected with $E(k,L)$ via [26]

$$\Sigma^2(L) \; := \; \left\langle (n(L)-L)^2 \right\rangle = \sum_{k=0}^{\infty} (k-L)^2 E(k,L) \tag{17}$$

$$\gamma_1(L) \; := \; \frac{1}{\Sigma^2(L)^{3/2}} \left\langle (n(L)-L)^3 \right\rangle = \frac{1}{\Sigma^2(L)^{3/2}} \sum_{k=0}^{\infty} (k-L)^3 E(k,L) \tag{18}$$

$$\gamma_2(L) \; := \; \frac{1}{\Sigma^2(L)^2} \left\langle (n(L)-L)^4 \right\rangle - 3 = \frac{1}{\Sigma^2(L)^2} \sum_{k=0}^{\infty} (k-L)^4 E(k,L) - 3 \quad . \tag{19}$$

In fig.4 we present the results for $\Sigma^2(L), \gamma_1(L)$ and $\gamma_2(L)$ computed from the spectrum of the Hadamard–Gutzwiller ensemble (full curve) in comparison with the curves obtained from the functions $E(k,L)$ for the GOE (dotted curve) and GUE cases (dashed curve). The Poisson case is shown too. For $L < 1.1$, $\Sigma^2(L)$ is in perfect agreement with the GOE prediction, but then it falls below the GOE curve indicating a more rigid spectrum than that of GOE for $L > 1.1$. However, the skewness γ_1 and the excess γ_2 show no deviation from GOE with increasing L. The fall–off of γ_1 is too slow in comparison with GUE and agrees with the GOE case. However, for $L > 3$, for which the deviation from GOE should increase, the curves of the GOE and GUE spectra are nearly indistinguishable. Therefore, the deviation is unobservable within the statistical significance of our data. The same result is obtained for γ_2, where the minimum at $L \simeq 0.45$ is in agreement with GOE, and the oscillations of γ_2 for larger ranges in L are too small to look like that of the GUE predictions. The Poisson case, expected for integrable systems, is excluded in all three cases.

The results on the number statistics corroborate nicely our findings on the probabilities $E(k,L)$ in sect.IV.1, that the short range statistic is well described by the GOE predictions. Surprising, however, is at first sight the extremely small L interval ($0 \leq L \leq 1.1$) in which $\Sigma^2(L)$ agrees with the GOE prediction. In fig.10 we show $\frac{1}{2}\Sigma^2(L)$ in a larger range up to $L = 50$. It is seen that $\Sigma^2(L)$, apart from small oscillations, saturates very quickly at the value 0.6 for $L \to \infty$. But this is exactly the behaviour which is expected from eq.(10), which predicts

$$\Sigma^2_{\rm HGE}(L) \; \to \; \alpha_\infty \simeq 0.6 \quad \text{for} \; L \to \infty \quad . \tag{20}$$

(A derivation of this result will be given in sect.IV.5.) Thus a saturation of the widths $\alpha(k)$ of the probabilities $E(k,L)$ for $k \to \infty$ implies a saturation of $\Sigma^2(L)$ for $L \to \infty$. It is then clear that $\Sigma^2(L)$ has to fall below the GOE prediction above some L value. What is surprising, is the "precocious saturation", i. e. a saturation already at about $L = 3$. In sect.IV.5 we will present a nice explanation for the precocious saturation.

IV.3 Level Spacings

The nearest–neighbour level spacing $P(0,s)$ is the simplest statistic and therefore most often discussed in the context of statistical properties of quantal spectra of chaotic systems. Very good approximations to the GOE and GUE predictions are

$$\text{GOE} \quad : \quad P(0,s) = \; \frac{\pi}{2}\, s\, e^{-\frac{\pi s^2}{4}} \tag{21}$$

$$\text{GUE} \quad : \quad P(0,s) = \; \frac{32}{\pi^2}\, s^2\, e^{-\frac{4s^2}{\pi}} \quad , \tag{22}$$

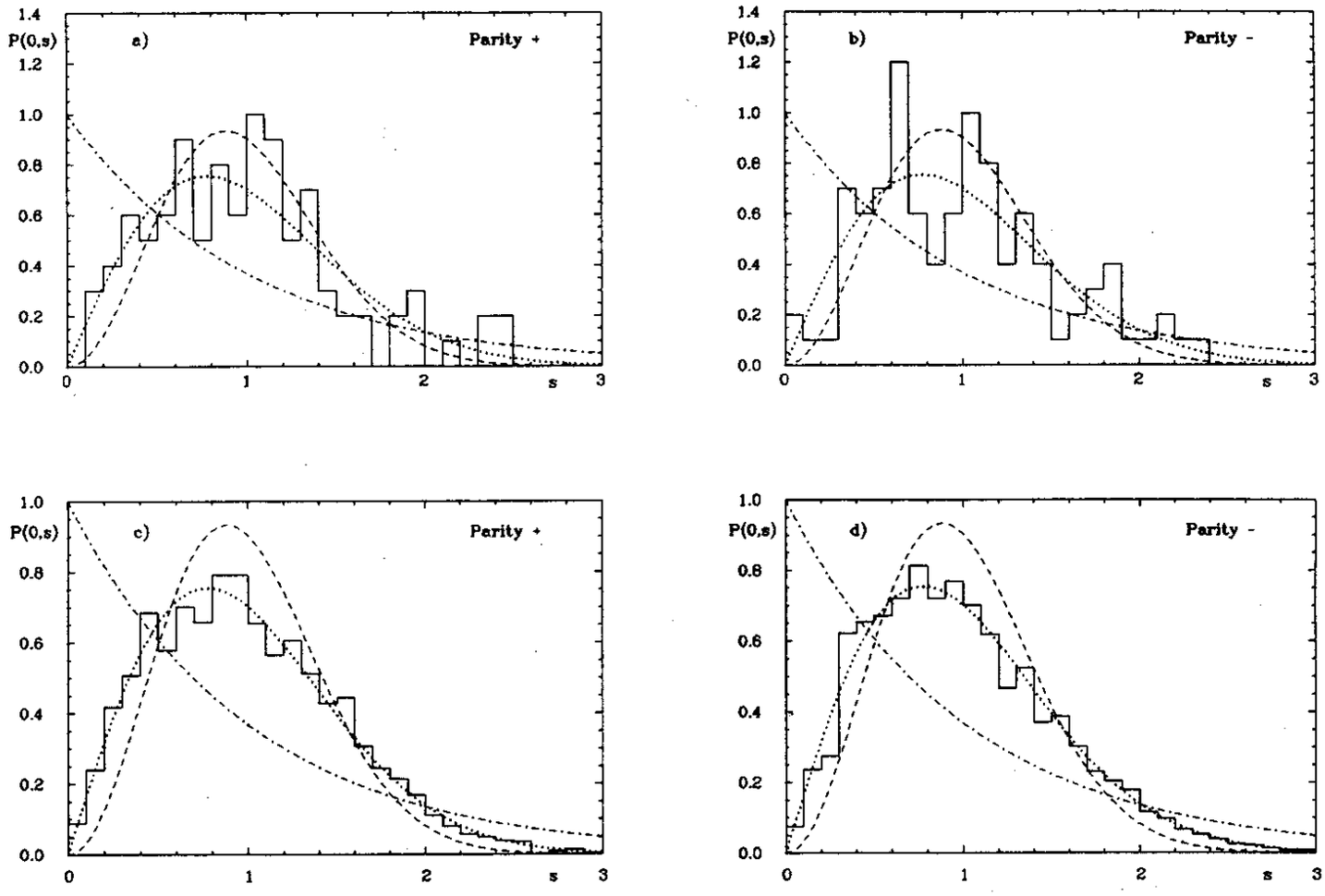

Figure 5: The level spacing $P(0,s)$ is presented for a single member of the Hadamard–Gutzwiller ensemble (a: parity + , b: parity −) and for the whole ensemble separated in parity classes (c: parity + , d: parity −) in comparison with the Poisson (chain curve), GOE (dotted curve) and GUE (dashed curve) predictions.

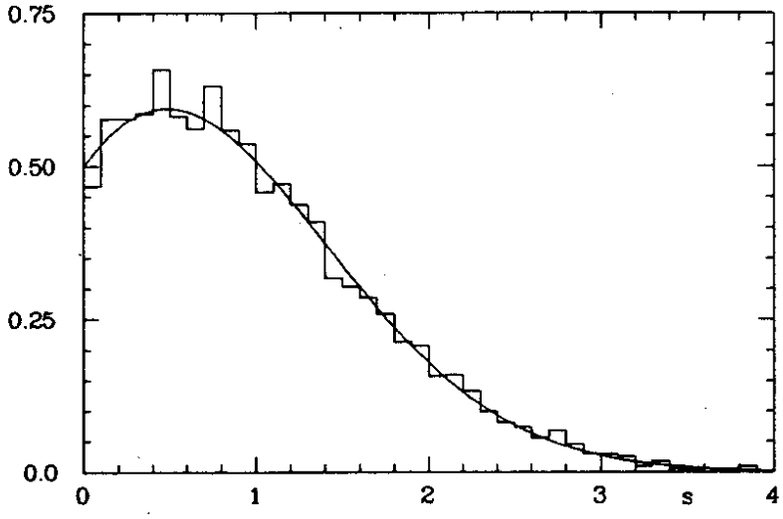

Figure 6: $\tilde{P}(s)$ for the Hadamard–Gutzwiller ensemble is shown in comparison with the expected distrubition (23) resulting from the superposition of two independent spectra obeying the Wigner distribution.

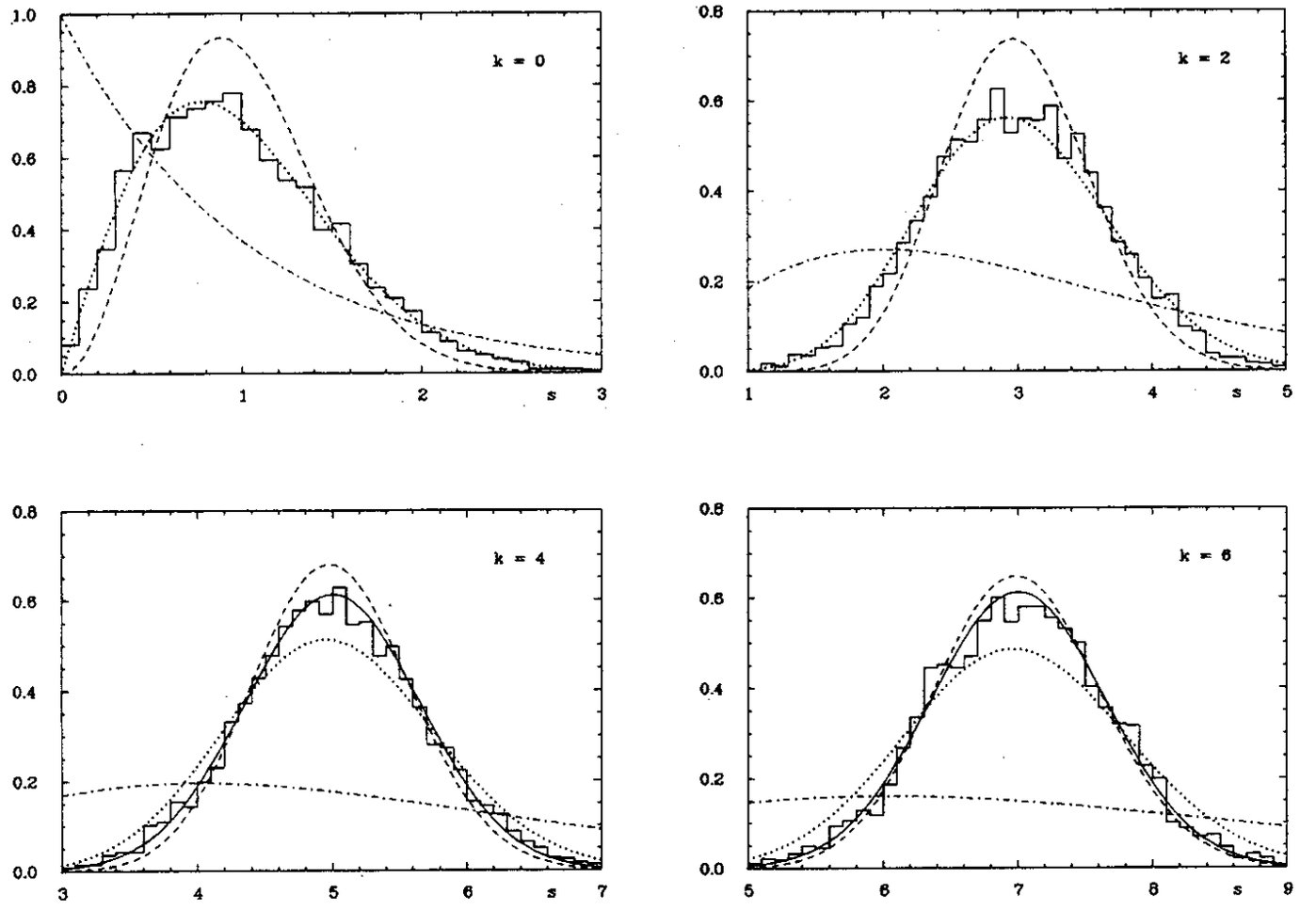

Figure 7: The four level spacings $P(k,s)$ for the cases $k = 0, 2, 4$ and 6 are presented in comparison with the Poisson (chain curve), GOE (dotted curve) and GUE (dashed curve) predictions. For the cases $k = 4$ and 6, we also show the results of our model (full curve), eq.(40).

where s is the spacing between two adjacent levels. For a Poisson distributed spectrum, one gets $P(0,s) = e^{-s}$.

It is important to check that the level–statistics for the Hadamard–Gutzwiller ensemble is the same for the two parity classes, which is expected if the statistical properties are assumed to be a common sign of chaos. To underscore that, fig.5 presents the level spacing $P(0,s)$ for a single system from our ensemble with parity classes considered separately (fig.5a,b), and for the whole ensemble again for the two parity classes (fig.5c,d). The statistic for the single system is based on 100 quantal energies, where we used a matrix of dimension 2500 in the method of finite elements. Its statistical significance is poor, of course, but it already points towards the GOE distribution and rules out a Poisson distributed spectrum. Figs.5 c and d demonstrate the large gain in statistical significance in using a whole ensemble instead of a single system. The agreement with the GOE prediction is very good; a GUE distribution is definitely ruled out. Thus we have shown that the first part of the rule, as proposed by Wigner for highly excited nuclei, holds for the Hadamard–Gutzwiller ensemble. The two parts of the rule may be formulated as follows [27]:

1. The spacing between adjacent levels having the same spin and parity is distributed (relative to the mean spacing) according to a frequency function which is given to a good approximation by the Wigner distribution (21).

2. The second part of the rule states that levels of different spin or parity are not in any way

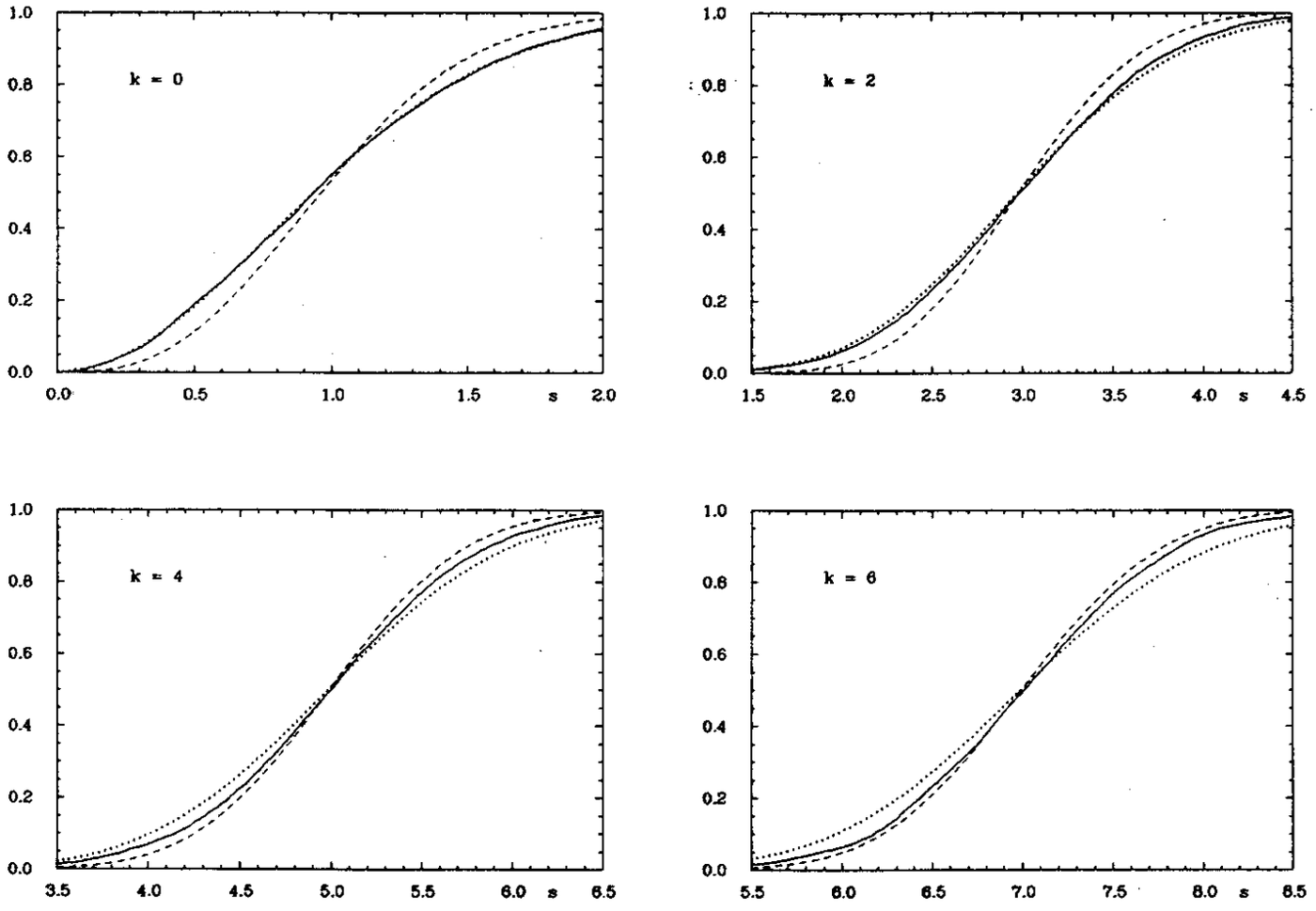

Figure 8: The cumulative level spacings $\int_0^s ds'\, P(k, s')$ are presented for $k = 0, 2, 4$ and 6 in comparison with the GOE (dotted curve) and GUE (dashed curve) predictions.

correlated in position. This has the consequence, that if one is dealing with a sequence of levels which is a superposition of sets of different spin or parity, the resulting distribution of spacing has a character which is intermediate between the Wigner distribution and the Poisson distribution.

Having shown that the even– and odd–parity levels separately obey the first part of the rule, we shall now show that the same levels are also in accord with the second part of the rule, i. e. that levels of different parity are not correlated in position. "This lack of correlation may be exhibited, for example, by considering the distribution of the spacings of *all* levels, no attention being paid to parity classification. Qualitatively, it is easily seen that a random superposition of two unrelated sequences leads to an increase in the number of small spacings. In the combined system of levels there will be a nonvanishing probability that a level of one sequence will be followed by a level of the other sequence. Since these two levels are assumed to be not correlated in any way, there will be a nonvanishing probability that the spacing between them is zero. Thus, we have the general result that the probability per unit interval for the occurrence of a zero spacing in the combined system of sequences will be nonvanishing." [27]

Let us consider the nearest–neighbour level spacing distribution for *all* levels of the Hadamard–Gutzwiller ensemble, no attention being paid to parity classification, which we denote by $\bar{P}(s)$. Since the two parity classes separately are in good agreement with the Wigner distribution (21), we expect $\bar{P}(s)$ to be described by a random superposition of the unrelated sequences, each governed by the Wigner distribution. The general problem of superposing two independent sequences was first

considered in ref.[28]. Specializing to the case of two Wigner distributions, we obtain the following distribution

$$\bar{P}(s) \;=\; \frac{\pi s}{8}\, e^{-\frac{\pi}{16}s^2}\, \mathrm{erfc}\left(\frac{\sqrt{\pi}}{4}s\right) \;+\; \frac{1}{2}e^{-\frac{\pi}{8}s^2} \quad . \tag{23}$$

(Note that $\bar{P}(s)$ has the properties $\bar{P}(0) = \frac{1}{2}$ and $\bar{P}'(0) = \pi/8$.) In fig.6 we plot $\bar{P}(s)$ for the Hadamard–Gutzwiller ensemble. The expected reduction of the repulsion of levels is quite evident. The distribution (23), represented by the continuous curve, is in excellent agreement with our numerical results.

We have already seen, that our spectrum deviates from the GOE predictions for greater spacings $s \equiv L$. To investigate the long–range statistics in more detail, we also consider the higher level spacings $P(k,s)$ for $k = 2, 4$ and 6, where $P(k,s)$ denotes the level spacing between two levels with k additional levels between them. The expectation value is

$$\langle s \rangle_k \;:=\; \int_0^\infty ds\; s\; P(k,s) \;=\; k \;+\; 1 \quad , \tag{24}$$

because of the normalization of the spectrum.

In fig.7 we show $P(k,s)$ for $k = 0, 2, 4$ and 6 in comparison with the GOE, GUE and Poisson predictions. For the Poisson case one gets [26]

$$P(k,s) \;=\; \frac{s^k}{k!}\, e^{-s} \quad , \tag{25}$$

whereas no such simple formulae exist for GOE and GUE. The latter are computed numerically as outlined in [22]. As in the case of $E(k,L)$, one recognizes a nice agreement for $k = 0$ with the GOE curve (dotted curve), whereas for the higher k values one sees a clear deviation from the GOE prediction. This confirms our earlier findings that the spectrum of the HGE is more rigid than the GOE spectrum.

Because the histograms in fig.7 display statistical fluctuations, it is more instructive to consider the integrated measure, i. e. the cumulative level spacing $\int_0^s ds'\, P(k,s')$, which is shown in fig.8 again for the cases $k = 0, 2, 4$ and 6. Here the striking agreement for $k = 0$ with the GOE curve is impressive, whereas for $k = 6$ the result is closer to the GUE prediction. In sect.IV.5 we will give a simple expression for the higher level spacings $P(k,s)$, which explains their behaviour in terms of the single parameter α_∞.

IV.4 Spectral Rigidity

As the last spectral measure, let us discuss the spectral rigidity $\Delta_3(L)$ introduced by Dyson and Mehta [21] as the average of the mean square deviation of the staircase $N(E) = \#\{E_n | E_n \leq E\}$ from the best fitting straight line $a + b\varepsilon$:

$$\Delta_3(L) := \left\langle \min_{(a,b)} \frac{1}{L} \int_{-L/2}^{L/2} d\varepsilon\, [N(E+\varepsilon) - a - b\varepsilon]^2 \right\rangle \quad , \tag{26}$$

where $\langle\ \rangle$ denotes a local average. This statistic measures more directly the rigidity of the spectrum than the level spacings $P(k,s)$. Our results for the Hadamard–Gutzwiller ensemble are shown in fig.9 and 10. One observes excellent agreement with the GOE prediction for $L < 8$. Knowing the behaviour of $E(k,L)$ and $P(k,s)$, it is no surprise to see, that the spectral rigidity $\Delta_3(L)$ displays for greater L's a more rigid behaviour than the GOE prediction.

The spectral rigidity $\Delta_3(L)$ is the only statistic, for which a theory exists, which was developed by Berry in [29] and is based on Gutzwiller's semiclassical periodic–orbit theory [19,20]. This theory predicts [29] for a system of 2 freedoms, that $\Delta_3(L)$ should display the following *universal behaviour*

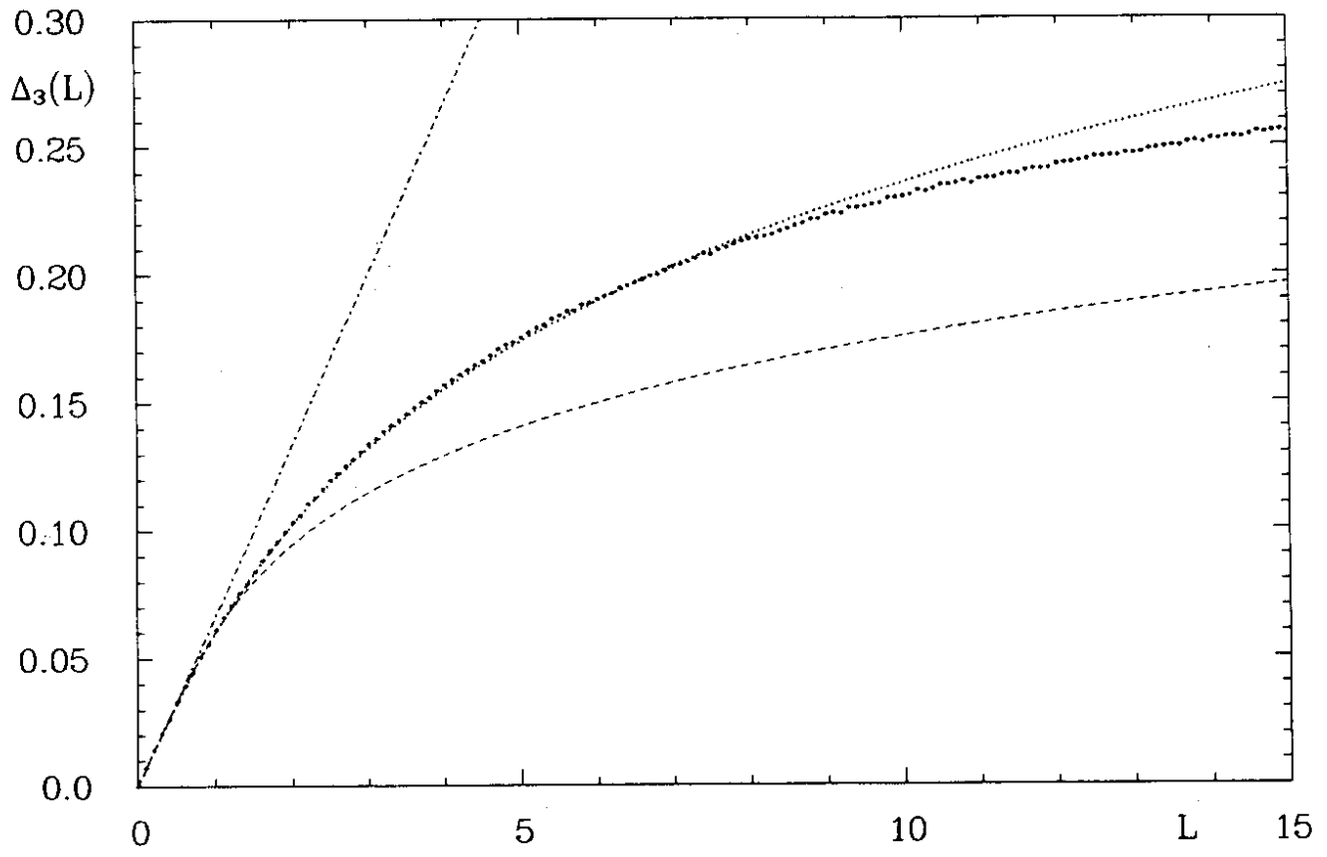

Figure 9: The spectral rigidity $\Delta_3(L)$ for the Hadamard–Gutzwiller ensemble (dots) is displayed in comparison with the GOE (dotted curve), GUE (dashed curve) and Poisson (chain curve) predictions.

as a result of properties of very long classical orbits: if the system is classically integrable (all periodic orbits filling tori), $\Delta_3(L) = \frac{1}{15}L$ (as in an uncorrelated Poisson eigenvalue sequence); if the system is classically chaotic (all periodic orbits are isolated and unstable) and has no symmetry, $\Delta_3(L) = \frac{1}{2\pi^2}\ln L + 0.0590$ if $1 \ll L \ll L_{\max}$ (as in the GUE of random-matrix theory); if the system is chaotic and has time-reversal symmetry, $\Delta_3(L) = \frac{1}{\pi}\ln L - 0.00695$ if $1 \ll L \ll L_{\max}$ (as in the GOE). When $L \gg L_{\max}$, however, $\Delta_3(L)$ saturates *non-universally* at a value, determined by short classical periodic orbits, of order $\hbar^{-1}$ for integrable systems and $\ln(\hbar^{-1})$ for chaotic systems. Here $L_{\max}$ corresponds to an "outer energy scale" which is determined by the shortest classical periodic orbit having period $T_{\min}$, $L_{\max} = 2\pi/T_{\min}$. (We have put again $\hbar =< d >^{-1} = 1$, where $< d >^{-1}$ is the mean level spacing.) For a given member of the Hadamard–Gutzwiller ensemble corresponding to a given octagon F, we have $T_{\min}(F) = l_0(F)/2p$, where $p = \sqrt{E - 1/4}$ denotes the momentum and $l_0(F)$ the length of the shortest periodic orbit on F. We thus obtain for the outer energy scale of the Hadamard–Gutzwiller ensemble

$$L_{\max}^{\mathrm{HGE}} \simeq \frac{4\pi}{l_0^{\mathrm{HGE}}}\sqrt{E} \quad , \tag{27}$$

where l_0^{HGE} plays the role of an *effective shortest length* corresponding to an ensemble average over the lengths $l_0(F)$ of the individual members of the HGE. For the octagons considered by us, the lengths $l_0(F)$ vary roughly between 1 and 3. With $l_0^{\mathrm{HGE}} \lesssim 3$ we arrive at the following *lower bound* $L_{\max}^{\mathrm{HGE}} \gtrsim (4\pi/3)\sqrt{E} \gtrsim 25$. To obtain the last number, we have inserted $E = 37.5$ which is the lowest energy E satisfying the condition $E - \widehat{L}/2 \geq 0$, if $\widehat{L} = 75$ denotes the upper bound of the interval $[0, \widehat{L}]$ over which the local average is taken in eq.(26). According to the semiclassical theory [29] we thus predict that the rigidity $\Delta_3(L)$ should display for $1 \ll L \ll 25$ the universal behaviour

$$\Delta_3(L) \simeq \Delta_3^{\mathrm{GOE}}(L) \simeq \frac{1}{\pi^2}\ln L - 0.00695 \tag{28}$$

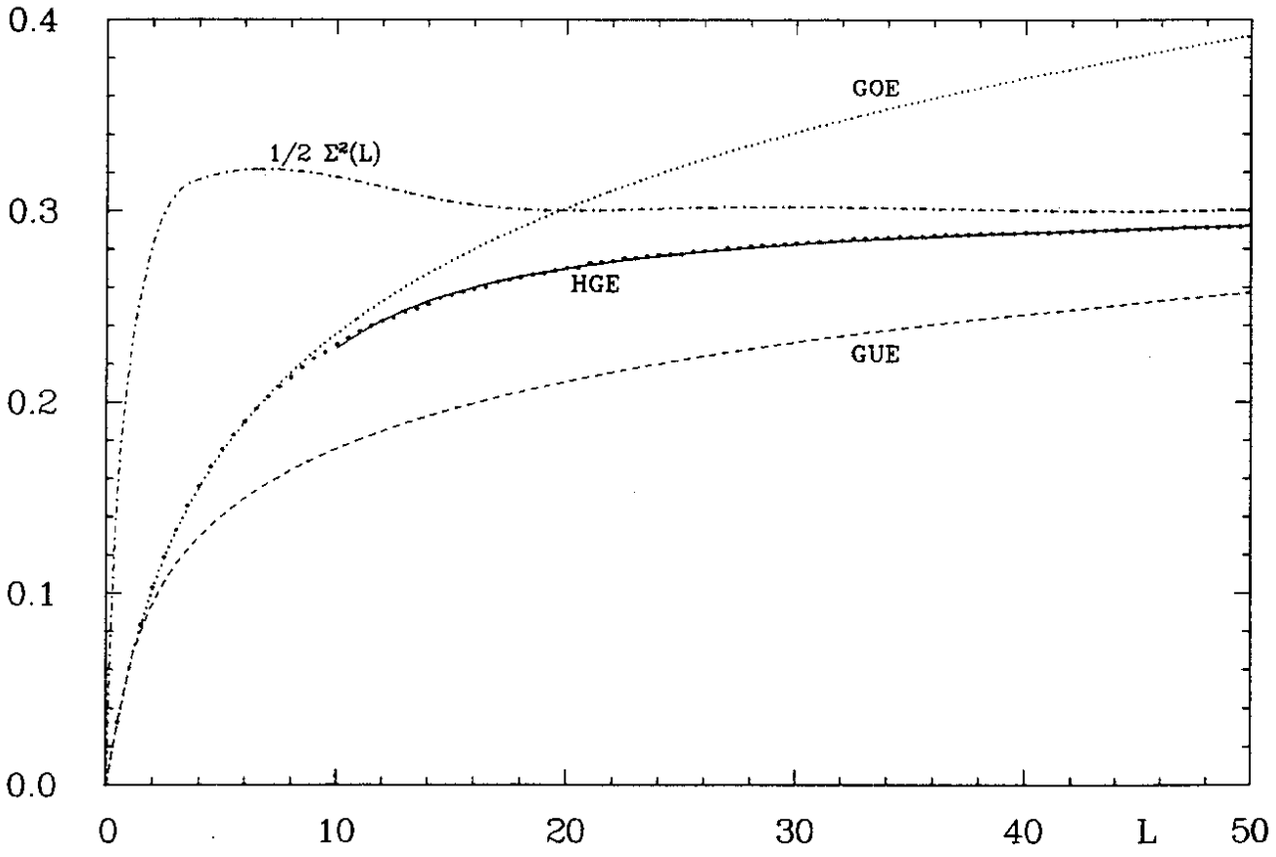

Figure 10: The spectral rigidity $\Delta_3(L)$ for the Hadamard–Gutzwiller ensemble (dots) is displayed for $L < 50$ in comparison with the GOE (dotted curve) and GUE (dashed curve) predictions. The full curve shows a best fit to $\Delta_3(L)$ using eq.(30). In addition $\frac{1}{2}\,\Sigma^2(L)$ is shown, because $\frac{1}{2}\Sigma^2(L) \simeq \Delta_\infty$ should be valid for $L \to \infty$.

which is consistent with our findings presented in figs.9 and 10 which show that the GOE prediction holds for $0 \leq L \leq 8$. When $L \gg L_{\max}$, the theory predicts that the rigidity saturates non–universally, at a value approximately given by [29]

$$\Delta_\infty \;=\; \frac{1}{\pi^2}\ln(e\,L_{\max}) \;-\; \frac{1}{8} \quad . \tag{29}$$

Using the above estimate $L_{\max}^{\rm HGE} \gtrsim 25$, we infer that $\Delta_3(L)$ for the HGE should saturate for $L \gg 25$ at a value $\Delta_\infty > 0.30$. A look at fig.10 shows, indeed, that $\Delta_3(L)$ seems to saturate at a value $\Delta_\infty > 0.29$. In order to get a better estimate for the saturation value Δ_∞, we have made a best fit to $\Delta_3(L)$ in the interval $10 \leq L \leq 60$ using the simple ansatz

$$\Delta_3(L) = \Delta_\infty \left[1 - \frac{a_1}{L} - \left(\frac{a_2}{L}\right)^2\right] \quad . \tag{30}$$

It can be seen from the full curve in fig.10 that (30) describes well for $L \geq 10$ the rigidity of the HGE, where the parameters turn out to be given by $\Delta_\infty = 0.305$, $a_1 = 2.115$, $a_2 = 2.048$. We thus conclude that the rigidity of the HGE saturates at a value $\Delta_\infty = 0.305$ which is completely consistent with the theoretical lower bound of 0.30.

It is worth remarking that the rigidity shows "slow saturation", reflected by the fact that $a_1 \neq 0$ in eq.(30), in contrast to the number variance $\Sigma^2(L)$, which shows a "precocious saturation" (see sect.IV.2). We shall explain this difference in behaviour in the next section.

Altogether it appears that the semiclassical theory gives a consistent description of the spectral rigidity. Recently, Berry [30] remarked "that the transition from universal to non–universal spectral statistics has not yet been seen in any honestly quantum Hamiltonian with a chaotic classical limit,

because not enough eigenvalues have been computed (the transition has been seen for an integrable system [29])." To the best of our knowledge, the results reported in this paper for the HGE demonstrate for the first time that this transition from universal to non–universal spectral statistics indeed occurs in an honestly chaotic system.

The theoretical understanding of $\Delta_3(L)$ yields immediately a *qualitative* understanding of the results for $E(k,L)$ and $P(k,s)$ presented in the previous sections. It is the purpose of the next section to show that the saturation of $\Delta_3(L)$ explains also *quantitatively* the observed behaviour of $E(k,L)$ and $P(k,s)$, and thus leads to a coherent picture of the energy–level statistics of the HGE.

IV.5 Consequences from the Saturation of the Spectral Rigidity

Let us now discuss the consequences for the spectral statistics which can be drawn from the existence of a finite saturation value Δ_∞. We start with a discussion of the number statistic $\Sigma^2(L)$. The relation between $\Delta_3(L)$ and $\Sigma^2(L)$ is given by a Volterra integral equation of the first kind for $\Sigma^2(L)$

$$L^4\,\Delta_3(L) \;=\; 2\int_0^L \left(L^3 - 2L^2 r + r^3\right)\Sigma^2(r)\,dr \quad . \tag{31}$$

Differentiating eq.(31) four times with respect to L and then considering the limit $L \to \infty$, where we can set $\Delta_3(L) = \Delta_\infty$, yields the inhomogeneous Euler differential equation

$$L^2\frac{d^2\Sigma^2(L)}{dL^2} + 2L\frac{d\Sigma^2(L)}{dL} - 6\Sigma^2(L) \;=\; -12\,\Delta_\infty \;,\; L \gg L_{\max} \;. \tag{32}$$

It has the general solution

$$\Sigma^2(L) \;=\; 2\,\Delta_\infty + c_1 L^2 + c_2 L^{-3}$$

where one must set $c_1 = 0$ for otherwise $\Sigma^2(L)$ would increase quadratically for $L \to \infty$. Then one gets $\Sigma^2(L) = 2\,\Delta_\infty + O(L^{-3})$ for $L \to \infty$. Thus we learn that the theoretically derived and numerically observed saturation of $\Delta_3(L)$ necessarily leads to a similar saturation of $\Sigma^2(L)$, where the saturation value Σ^2_∞ is given by the simple relation

$$\Sigma^2_\infty \;=\; 2\,\Delta_\infty \quad . \tag{33}$$

A look at fig.10 reveals, that a saturation value of $\Delta_\infty \simeq 0.3$ explains well the saturation value $\simeq 0.6$ of $\Sigma^2(L)$. To demonstrate the validity of eq.(33), we show $\frac{1}{2}\Sigma^2(L)$ in fig.10, too. This curve has been smoothed because $\Sigma^2(L)$ for the individual members of the HGE shows for $L > L_{\max}(F)$ quasirandom oscillations which non–universally depend on the individual length spectrum. Oscillations of this kind have been found by Odlyzko [31] and theoretically explained by Berry [30] for the number variance of the Riemann zeros. For a given member of the HGE, $\Sigma^2_\infty(F) = \frac{2}{\pi^2}\ln(eL_{\max}(F)) - \frac{1}{4}$ plays the role of the *mean value* about which the quasirandom oscillations take place. Since the oscillations are quasirandom, they should cancel in the ensemble average. We observe such a cancellation for the HGE, but it is still incomplete due to the limited number of octagons considered in our analysis.

The relation (31) explains also the observed "precocious saturation" of $\Sigma^2(L)$ versus the "slow saturation" of $\Delta_3(L)$. Knowing the asymptotic expansion (30), it is easy to derive from (31) that $\Sigma^2(L)$ still obeys $\Sigma^2(L) = \Sigma^2_\infty + O(L^{-3})$. But the absence of $O(L^{-1})$ and $O(L^{-2})$ terms implies precocious saturation of $\Sigma^2(L)$.

Having derived the interesting relation (33) between the number variance $\Sigma^2(L)$ and the rigidity $\Delta_3(L)$, which must hold in general for strongly chaotic systems, one can ask whether a similar relation exists also for the GOE and GUE predictions of random–matrix theory. Writing the asymptotic expansions (11) and (12) in the form $\Sigma^2(L) = A\ln L + B + O(L^{-2})$, one easily derives from (31) for $L \gg 1$

$$\Sigma^2(L) \;=\; 2\,\Delta_3(L) + \frac{9}{4}A + O(L^{-1}) \tag{34}$$

with $A = \frac{2}{\pi^2}$ for GOE and $A = \frac{1}{\pi^2}$ for GUE, which is the natural generalization of (33).

Let us now come to the functions $E(k,L)$, whose connection with $\Sigma^2(L)$ is given by eq.(17). Table 2 shows, that for $k > 3$ the function $\alpha(k)$ of the ansatz

$$E(k,L) = \frac{1}{\sqrt{2\pi\alpha(k)}}\, e^{-\frac{(k-L)^2}{2\alpha(k)}} \tag{35}$$

is approximately constant at $\alpha(k) \simeq \alpha_\infty = 0.615$. This can be understood in terms of the saturation value Δ_∞, too. Using the Euler–MacLaurin summation formula, one gets for $L \to \infty$

$$\begin{aligned} 2\,\Delta_\infty \simeq \Sigma^2(L) \simeq \sum_{k=4}^{\infty}(k-L)^2\,\frac{1}{\sqrt{2\pi\alpha_\infty}}e^{-\frac{(k-L)^2}{2\alpha_\infty}} &\simeq \int_3^\infty dk\,(k-L)^2\frac{1}{\sqrt{2\pi\alpha_\infty}}e^{-\frac{(k-L)^2}{2\alpha_\infty}} \\ &= \frac{1}{\sqrt{2\pi\alpha_\infty}}\int_{3-L}^{\infty} dy\; y^2\, e^{-\frac{y^2}{2\alpha_\infty}} \\ &\to \frac{1}{\sqrt{2\pi\alpha_\infty}}\int_{-\infty}^{\infty} dy\; y^2\, e^{-\frac{y^2}{2\alpha_\infty}} = \alpha_\infty \end{aligned}$$

and therefore

$$\alpha_\infty = 2\Delta_\infty \quad . \tag{36}$$

Strikingly, the value $\Delta_\infty = 0.305$ yields $\alpha_\infty = 0.610$, which agrees nicely with our numerical value. Combining eqs.(33) and (36), we obtain (20), which was already found in sect.IV.2 to be in nice agreement with our numerical results.

In sect.IV.1 we have shown that the ansatz (35) gives for $k > 3$ an excellent fit also to the GOE and GUE predictions, where $\alpha(k)$, however, does not saturate for $k \to \infty$ at a finite value, but rather increases logarithmically. For $\alpha(k) = a\ln k + b$ $(a, b > 0)$ (see eq.(13)) we have checked numerically that the relation

$$\int_3^\infty dk\,(k-L)^2\,\frac{e^{-\frac{(k-L)^2}{2\alpha(k)}}}{\sqrt{2\pi\alpha(k)}} \simeq \alpha(L) \tag{37}$$

holds for $L \to \infty$. Thus the same argument as above, using the Euler–MacLaurin summation formula, can be applied to derive for GOE and GUE

$$\Sigma^2(L) \simeq \alpha(L) \quad , \quad L \gg 1 \quad , \tag{38}$$

a result which we anticipated in eq.(10) and already checked in table 3.

Finally, let us discuss the level spacings $P(k,s)$, which are given by [22]

$$P(k,s) = \sum_{j=0}^{k}(k+1-j)\,\frac{d^2\,E(j,s)}{ds^2} \quad . \tag{39}$$

For $k > 3$, $E(k,s)$ are determined by eq.(35) with $\alpha_\infty = 2\Delta_\infty$, and therefore $P(k,s)$ are determined in turn by

$$P(k,s) \simeq \frac{1}{\sqrt{16\pi\,\Delta_\infty^3}}\sum_{j=0}^{k}(k+1-j)\left(\frac{(j-s)^2}{2\Delta_\infty}-1\right)e^{-\frac{(j-s)^2}{4\Delta_\infty}} \quad . \tag{40}$$

Eq.(40) has been derived for $s \to \infty$, but it does its job well for $k > 2$, $s > 2$! After evaluating eq.(40) numerically using our value $\Delta_\infty = 0.305$, we fit the result with the Gaussian

$$P(k,s) = \frac{1}{\sqrt{2\pi\sigma}}e^{-\frac{(s-k-1)^2}{2\sigma^2}} \quad , \tag{41}$$

which yields already for $k > 3$ the constant value $\sigma_\infty = 0.659$, i.e. a saturation value Δ_∞ forces $P(k,s)$ to be a Gaussian centered at $s = k+1$ with a constant width σ_∞. On the other hand, we can fit

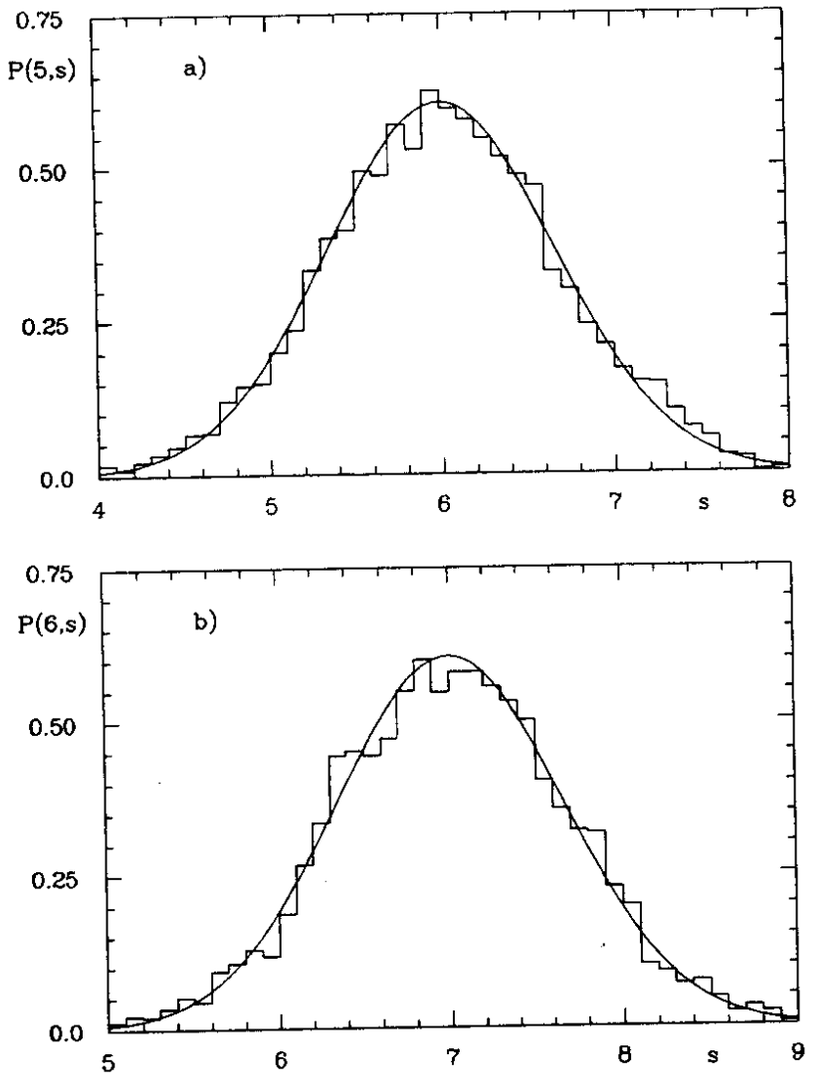

Figure 11: P(k,s) for a) $k = 5$ and b) $k = 6$ is shown in comparison with eq.(40) for $\Delta_\infty = 0.305$.

eq.(41) directly to the data for the HGE. For $k > 3$ we obtain nice fits with $0.67 < \sigma < 0.68$, i. e. with σ–values slightly larger than the value $\sigma_\infty = 0.659$. One must keep in mind, however, that the data are given as histograms (see fig.7) and thus yield less precise fit parameters. To demonstrate the astonishing agreement despite of the small numerical uncertainty, we present in fig.11 $P(k,s)$ for the cases $k = 5$ and $k = 6$ in comparison with eq.(40) using $\Delta_\infty = 0.305$.

Independent of the ansatz (41), we can define the variance $\sigma^2(k)$ of s using the general definition

$$\sigma^2(k) := < s^2 >_k - < s >_k^2 \quad , \quad k = 0, 1, 2, \ldots \quad , \tag{42}$$

where

$$< s^n >_k := \int_0^\infty ds\, s^n\, P(k,s) \tag{43}$$

(see also eq.(24)). Using eq.(39) and performing two partial integrations, it is straightforward to derive the following relationship between $\sigma^2(k)$ and the integrals $I(k)$ introduced in eq.(14) [25]

$$\sigma^2(k) = 2 \sum_{j=0}^{k} (k+1-j)\, I(j) - (k+1)^2 \quad . \tag{44}$$

It follows from the last equation, that the two sets $\{\sigma(k)\}$ and $\{I(k)\}$ are not independent from each other, since a knowledge of $I(j)$ for $j = 0$ to k determines uniquely $\sigma^2(j)$ for $j = 0$ to k. In sect.IV.1 we mentioned already that the Gaussian approximation (35) predicts $I(k) = 1$ for $k \geq K$, if (35) is assumed to be valid for $k \geq K$, and we inferred from a fit to the functions $E(k,L)$ the value $K = 4$ for the HGE. This prediction was nicely confirmed in table 4, which, taken literally, yields $K = 5$, but

which is consistent in fact with $K = 4$ since the deviation of $I(k)$ from our prediction is only 0.004, and we do not claim that our numerical values are precise at the level 10^{-3}. Assuming $I(k) = 1$ for $k \geq K$, we obtain from eq.(44) for $k \geq K$

$$\sigma^2(k) \;=\; 2k \left\{ \sum_{j=0}^{K-1} I(j) - \left(K - \frac{1}{2} \right) \right\} \;+\; K(K-3) + 1 \;-\; 2 \sum_{j=0}^{K-1} (j-1) I(j) \quad . \tag{45}$$

Without further input, eq.(45) predicts for $\sigma^2(k)$ a linear increase in k, which contradicts the asymptotic saturation at a value σ^2_∞. In order to be consistent with the observed saturation, the curly bracket in eq.(45) must vanish, which leads to the sum rule

$$\sum_{k=0}^{K-1} I(k) \;=\; K - \frac{1}{2} \quad . \tag{46}$$

Using for $I(k)$ the values given in table 4 for the HGE, we obtain for the left–hand side of eq.(46) the values 3.508 and 4.504 for $K = 4$ and 5, respectively, which shows that the sum rule is satisfied within our numerical accuracy.

Assuming the exact validity of the sum rule (46), we derive from eq.(45) the following relation for the saturation value σ^2_∞

$$\sigma^2_\infty \;=\; K(K-1) \;-\; 2 \sum_{k=1}^{K-1} k\, I(k) \quad . \tag{47}$$

With the values given in table 4 for the HGE and for $K = 5$ we obtain from (47) the saturation value $\sigma_\infty = 0.645$ which is quite consistent with the value 0.659 obtained from eq.(40). Relation (47) shows explicitly that σ^2_∞ is very sensitive against small changes in $I(k)$. For example, if we change just the integral $I(4)$ by the tiny amount -0.004 (i.e. $I(4) \rightarrow 0.992$, see table 4), which renders the sum rule (46) to be *exact* for $K \geq 5$, we get a change in σ^2_∞ by $+0.032$ yielding the new value $\sigma_\infty = 0.669$.

The above discussion has shown that a saturation of $\Delta_3(L)$ at a value Δ_∞ is accompanied by a saturation of $\sigma^2(k)$ at a value σ^2_∞ as a consequence of eq.(40). For the other statistics we have discussed before how they depend on the saturation parameter Δ_∞, and we were led to the remarkable relations (20),(33) and (36). It is suggestive to ask whether there exists a similar relation connecting σ^2_∞ with Δ_∞, i.e. with Σ^2_∞. To answer this question, we display in table 5 the values for σ_∞ obtained from a fit of eq.(41) to eq.(40) for Δ_∞ varying in steps of 0.05 between 0.25 and 0.70. In addition, we show the combination $2\Delta_\infty - \sigma^2_\infty$. With (33) we are thus led to the relation

$$\Sigma^2_\infty \;=\; \sigma^2_\infty \;+\; \rho \quad , \tag{48}$$

where ρ is roughly constant, i.e. $0.17 \leq \rho \leq 0.18$ for $0.50 \leq \Sigma^2_\infty \leq 1.40$. Relation (48) is reminiscent of a similar relation [6] connecting $\Sigma^2(L)$ and $\sigma^2(k)$ for the GOE and GUE, where ρ has been predicted [32] to have the value $\frac{1}{6}$, while the exact result gives for GOE $0.16 \leq \rho \leq 0.17$ for $0 \leq k \leq 7$, which is very similar to the values obtained by us for the HGE.

Δ_∞	0.25	0.30	0.35	0.40	0.45	0.50	0.55	0.60	0.65	0.70
σ_∞	0.565	0.651	0.725	0.792	0.853	0.910	0.964	1.015	1.063	1.109
$2\Delta_\infty - \sigma^2_\infty$	0.181	0.176	0.174	0.173	0.172	0.172	0.171	0.170	0.170	0.170

Table 5: The dependence of σ_∞ in eq.(41) on the saturation value Δ_∞ of the spectral rigidity.

V Discussion

A big unsolved problem in quantum chaology is to find an explicit semiclassical quantization condition for the *individual* energy levels of classically chaotic systems. Although Gutzwiller's periodic–orbit theory [19,20] leads to very interesting sum rules [17,18] for the quantal energies, it does not provide – at least in its present form – such a quantization condition. It is true, that by computing a huge number of periodic orbits, we could demonstrate recently for the symmetrical Hadamard–Gutzwiller model [17,18] and for the hyperbola billiard [33] that a Gaussian smoothing of the periodic–orbit sum allows indeed a determination of the *low–lying* energy levels. But even with millions of periodic orbits, we were unable to recover *high excited* levels. Lacking an explicit semiclassical quantization rule for the individual energy levels, one is led to study the *statistics* of the levels.

In this paper we have presented for the Hadamard–Gutzwiller ensemble, considered as a model for quantum chaology, a detailed statistical analysis of the *fluctuations* of the energy levels about the mean level density.

The results reported in this paper demonstrate clearly that the energy–level statistics of the Hadamard–Gutzwiller model, defined on a *generic asymmetric* octagon, are (after parity separation) in complete agreement with the short–range statistics of random–matrix theory (see figs.5a) and b)). We have thus shown for the first time, that the motion on compact Riemann surfaces provides a generic model for quantum chaology.

In order to improve the statistical significance, we have studied instead of a single model a whole *ensemble* of different Hadamard–Gutzwiller models, called the Hadamard–Gutzwiller ensemble. Studying 30 different asymmetric octagons provided us, after parity separation, with 60 different level sequences comprising altogether 4500 energy levels. Based on this relatively large sample, we were able to study in detail various fluctuation measures.

The results obtained for the different measures led us to a coherent picture of the energy–level statistics of the HGE: the short–range statistics of the quantal energies E_n are in perfect agreement with the GOE predictions of random–matrix theory as first surmised by Wigner and by Landau and Smorodinsky for nuclear level statistics. Thus our results strengthen the hypothesis, that quantum systems with chaotic classical counterpart display level repulsion as predicted by random–matrix theory. On the other hand, the level statistics describing correlations over greater level distances deviate from the GOE predictions. But this non–universal behaviour can be uniquely described as a "saturation effect" caused by the shortest periodic orbits of the HGE. According to the semiclassical theory developed by Berry [29], the rigidity $\Delta_3(L)$ saturates at a value Δ_∞ given approximately by eq.(29). One of the main results of this paper is the fact that a similar saturation is observed also for the other fluctuation measures, viz. the "width" $\alpha(k)$, the number variance $\Sigma^2(L)$ and the variance $\sigma^2(k)$, and, furthermore, that all those measures saturate at values which are completely determined by the single parameter Δ_∞

$$\alpha_\infty \;=\; \Sigma^2_\infty \;=\; 2\,\Delta_\infty \;=\; \sigma^2_\infty \,+\, \rho \quad . \tag{49}$$

(Of course, a good answer to the question "Who needs ρ?" has yet to be given, though the "correction" $\rho \simeq 0.17 - 0.18$ is uniquely determined by eqs.(40) and (41).) Since all fluctuation measures studied in this paper can be derived from the probabilities $E(k,L)$, we cite again eq.(8)

$$E(k,L) \;=\; \frac{1}{\sqrt{2\pi\Sigma^2_\infty}}\, e^{-\frac{(L-k)^2}{2\Sigma^2_\infty}} \quad , \quad k \geq 4 \;, \tag{50}$$

expressed now in terms of the single parameter

$$\Sigma^2_\infty \;=\; \frac{2}{\pi^2}\ln(eL_{\max}) - \frac{1}{4} \quad . \tag{51}$$

It is worth mentioning that eq.(50) has not been derived from semiclassical theory, but rather we have shown that the simple Gaussian ansatz (50) describes well the long–range statistics of all the

fluctuation measures and is, furthermore, *consistent* with the predictions of the semiclassical theory, since from eq.(50) we can *derive* the saturation of $\Delta_3(L)$ and $\Sigma^2(L)$.

To our knowledge, it is the first time that the transition from universal to non–universal spectral statistics has been seen in an honestly quantum Hamiltonian with a chaotic classical limit.

There remains to test the *energy–dependence* of the various saturation values. E.g. for Σ^2_∞ we obtain from eq.(27) and (51) the prediction

$$\Sigma^2_\infty \;=\; \frac{1}{\pi^2}\ln E \;+\; \frac{2}{\pi^2}\ln\left(\frac{4\pi e}{l_0^{\overline{\mathrm{HGE}}}}\right) \;-\; \frac{1}{4} \quad , \tag{52}$$

where E is the energy near to which the average over the energy intervals of length L is carried out in the computation of $\Sigma^2(L)$. Unfortunately, the energy interval, which was attainable to us in this paper, is too small to carry out the required test. Notice, however, that eq.(52) predicts that in the genuine semiclassical limit, $E \to \infty$, Σ^2_∞ increases without limit, which implies that the GOE–curve for $\Sigma^2(L)$ plays the role of an envelope to which the "experimental" number variance converges. In this sense the GOE prediction of random–matrix theory is asymptotically recovered.

After completion of this paper we became aware of Berry's lectures [34], where "some issues that lie at the foundations" of quantum chaology are well discussed. In these lectures the semiclassical theory is extended to the number variance $\Sigma^2(L)$.

Acknowledgement

We would like to thank the Deutsche Forschungsgemeinschaft for financial support and the HLRZ at Jülich for the access to the CRAY–YMP computer. We are grateful to M.L.Mehta for providing us with a reprint of [22] and to Martin Sieber for drawing our attention to ref.[34].

References

[1] M.V.Berry and M.Tabor, Proc. Roy. Soc. London, Ser. **A356**(1977) 375.

[2] G.M.Zaslavskii, Zh. Eksp. Teor. Fiz. **73**(1977) 2089 ; Sov. Phys. JETP **46**(1977) 1094.

[3] O.Bohigas, M.J.Giannoni and C.Schmit, Phys. Rev. Lett. **52**(1984) 1.

[4] C.E.Porter, Statistical Theories of Spectra : Fluctuations (Academic Press, New York, 1965).

[5] M.L.Mehta, Random Matrices and the Statistical Theory of Energy Levels (Academic Press, New York, 1967).

[6] T.A.Brody, J.Flores, P.A.Mello, A.Pandey and S.S.M.Wong, Rev.Mod.Phys. **53**(1981) 385.

[7] R.U.Haq, A.Pandey and O.Bohigas , Phys.Rev.Lett. **48**(1982) 1086; O.Bohigas, R.U.Haq and A.Pandey, Phys.Rev.Lett. **54**(1985) 1645.

[8] A.Abul–Magd and H.A.Weidenmüller, Phys. Lett. **162B**(1985) 223.

[9] T.H.Seligman and H.Nishioka (eds.), Quantum Chaos and Statistical Nuclear Physics, Lecture Notes in Physics **263**(1986).

[10] O.Bohigas, M.–J.Giannoni and C.Schmit , in ref. [9].

[11] M.V.Berry, Proc. Roy. Soc. London, Ser. **A413**(1987) 183.

[12] Th.Zimmermann, L.S.Cederbaum, H.–D.Meyer and H.Köppel, J. Phys. Chem. **91**(1987) 4446.

[13] B.Eckhardt, Phys. Rep. **163**(1988) 205.

[14] J.Hadamard, J. de Math. pure et appl. **4**(1898) 27.

[15] M.C.Gutzwiller, Phys. Rev. Lett. **45**(1980) 150; Physica Scripta **T9**(1985) 184; Contemp. Math. **53**(1986) 215.

[16] R.Aurich and F.Steiner , Physica **D32**(1988) 451.

[17] R.Aurich, M.Sieber and F.Steiner, Phys.Rev.Letters **61**(1988) 483.

[18] R.Aurich and F.Steiner, DESY Preprint 89–026 (March 1989), Physica **D** in print, to appear in December 1989.

[19] M. C. Gutzwiller, J. Math. Phys. **8**(1967) 1979, and **10**(1969) 1004, and **11**(1970) 1791, and **12**(1971) 343; in *Path Integrals and their Applications in Quantum, Statistical and Solid-State Physics*, edited by G. J. Papadopoulos and J. T. Devreese (Plenum, New York, 1978), p. 163; Physica **D7**(1983) 341.

[20] R. Balian and C. Bloch, Ann. Phys. (N.Y.) **69**(1972) 76, and **85**(1974) 514;
R. Dashen, B. Hasslacher, and A. Neveu, Phys. Rev. **D10**(1974) 4114;
M. V. Berry, in *Semiclassical Mechanics of Regular and Irregular Motion*, Proceedings of the Les Houches Summer School Session XXXVI, edited by G. Iooss, R. H. G. Helleman and R. Stora (North-Holland, Amsterdam, 1983), p. 171;
A. Voros, J. Phys. **A21**(1988) 685.

[21] F.J.Dyson and M.L.Mehta , J.Math.Phys. 4(1963) 701.

[22] M.L.Mehta and J.Des Cloizeaux, Ind. J. Pure Appl. Math. **3**(1972) 329.

[23] N.L.Balazs and A.Voros, Phys. Rep. **143**(1986) 109.

[24] R.Aurich and F.Steiner, to be published.

[25] O.Bohigas and M.J.Giannoni, Ann. Phys. (NY) **89**(1975) 393.

[26] O.Bohigas and M.–J. Giannoni, Springer Lecture Notes in Physics **209**(1984) 1.

[27] N.Rosenzweig and C.E.Porter, Phys. Rev. **120**(1960) 1698.

[28] A.M.Lane, Oak Ridge National Laboratory Report ORLN–2309, 1957 (unpublished); reprinted in [4].

[29] M.V.Berry, Proc. Roy. Soc. London, Ser.**A400**(1985) 229.

[30] M.V.Berry, Nonlinearity **1**(1988) 399.

[31] A.M.Odlyzko, Math. Comp. **48**(1987) 273.

[32] J.B.French, P.A.Mello and A.Pandey, Ann. Phys. (NY) **113**(1978) 277.

[33] M.Sieber and F.Steiner, DESY Preprint 89–093 (July 1989)

[34] M.V.Berry, Some quantum–to–classical asymptotics, Lectures given at the Les Houches school on Chaos and Quantum Physics (August 1989), to be published by North–Holland.